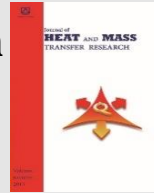




Semnan University



Research Article

Unsteady Heat Transfer in Cylindrical Encapsulated Phase Change Materials with Buoyancy Effect

Javad Rostami

Department of Mechanical Engineering, Faculty of Engineering, Razi University, Kermanshah, 6714414971, Iran

ARTICLE INFO

Article history:

Received: 2024-02-08

Revised: 2024-06-07

Accepted: 2024-06-07

Keywords:

PCM;

Convective heat transfer;

CFD;

Latent heat;

Sensible heat

ABSTRACT

In this paper, the effect of buoyancy force on the temperature change of the phase change materials which has been encapsulated in two pipes in a channel, is simulated numerically using Boussinesq approximation. An application of this topic is in air-conditioning, which uses ice in the pipes as PCM for coolant and the aim is calculating the PCM discharging time. The unsteady governing equations including continuity, momentum and energy in the fluid flow and phase change material for laminar flow regime, have been solved by the well-known SIMPLE method. The needed time to phase change material reach the inlet temperature of the fluid flow has been obtained and compared to the results of the lumped temperature assumption. The results show that the discharging time is 4,000 for $Gr=5,000$ and 70,000 for $Gr=200,000$. It is 25,000 for $k_r=0.5$ and 34,000 for $k_r=1.5$. Also, it is 11,000 for $Cp_r=10^3$ and 28,000 for $Cp_r=10^4$. Finally, it has been concluded that due to the fine mixing of PCM because of buoyancy force, the results are so closed to the results of the lumped temperature assumption for PCM.

© 2024 The Author(s). Journal of Heat and Mass Transfer Research published by Semnan University Press.

This is an open access article under the CC-BY-NC 4.0 license. (<https://creativecommons.org/licenses/by-nc/4.0/>)

1. Introduction

When the phase change materials are in phase change duration time, they are known as convenient feature materials in heat transfer technology. Because, in this period, when their temperature is constant, they act as a heat sink or heat source. But, after phase change duration, their temperature varies. With the advancement in the air conditioning field, the demand for energy saving has increased. One way to reduce energy consumption in buildings is to use phase change materials (PCMs). To do this, the chiller of the air handling unit is turned on during the hours of midnight when the electricity consumption is reduced. In this process, the water turns to ice inside the capsules located in

the air duct. Then, in the early hours of the morning, only the fan of the air conditioner (with low electricity consumption) is turned on to allow air to pass through these capsules and provide the needed cool air for the building. It was one of the PCMs application, but there are a lot of usage for them in industry. Then, many researchers are studying these materials.

Using PCM to save energy or delay the temperature peak has been evaluated in some research. The cooling behavior of a vertical plate in a phase change material/water composite enclosure under a pulsating heat load was studied by Ho and Cheng [1]. The PCM was n-octadecane, and the second fluid was water. The flow was laminar both in the PCM and in the

* Corresponding author.

E-mail address: jrostami@razi.ac.ir.

Cite this article as:

Rostami, J., 2024. Unsteady Heat Transfer in Cylindrical Encapsulated Phase Change Materials with Buoyancy Effect. *Journal of Heat and Mass Transfer Research*, 11(2), pp. 225-236.

<https://doi.org/10.22075/JHMTR.2024.33230.1522>

water. Their results reveal that the water layer has a better capability of heat dissipation than the PCM. Energy efficiency optimization of the waste heat recovery system with phase change materials has been studied by Yan et al. [2]. In this work, the exhaust gas from the building passes a heat exchanger, and its other fluid is the circulation air of the building. The PCM is located in the heat exchanger. They reported that using PCM increases the buildings fuel saving from 19% for without PCM to 48% with PCM using. Khan et al. [3] studied heat transfer of the building walls in the presence of PCM. Their results include both the melting and the duration of PCM after melting. In this study, two models of the building walls were investigated. In one model, they found an optimum state by changing the position of the PCM in the wall.

The effect of buoyancy-driven convection on melting within spherical or cylindrical containers is studied by [4-11]. Khodadadi and Zhang [4] claimed that at the initial time of melting in a spherical capsule, the conduction mechanism is dominant. But, by time increasing, due to buoyancy driven the convection effects has a main role in the heat transfer mechanism. Assis et al. [5] studied the PCM melting process in a spherical shell both experimentally and numerically. The PCM was paraffin wax which is used in latent heat, based storage system. Their results show that the transient melting process depends on the temperature difference between the wall, the mean melting temperature of the PCM, and the diameter of the shell. The melting process of PCMs inside a spherical capsule has been studied by Tan et al. [6]. In their study, the PCM was Paraffin wax n-octadecane. They investigated the role of the buoyancy driven convection during melting. Elmozughi et al. [7] analyzed heat transfer in encapsulated PCM for high temperature thermal energy storage. The PCM was sodium nitrate in the stainless-steel cover. In this study, the PCM is used to concentrate solar power applications, and different boundary conditions are applied for laminar and turbulent flows. Their results show that melting and solidification processes are differing due to presence of the buoyancy force in melting. Aadmi et al. [8] studied PCM melting in a horizontal tube of thermal energy storage. The effects of radius of the cylinder on the PCM melting has been studied. They investigated the effect of the radius of the pipes on the heat transfer rate. Their results cover both melting (isotherm) and after melting durations (temperature increasing). Zeneli et al. [9] simulated a silicon-based latent heat thermal energy storage system operating at ultra-high temperatures. The effect of the buoyancy driven force on the PCM melting is investigated. The

results revealed that a reduction in the melting time by 31% occurred when the Stefan number increased by 35%. Mallya and Haussener [10] studied the buoyancy-driven melting and solidification heat transfer in encapsulated PCM. They studied transient dynamic heat transfer behavior of different PCMs in different shape of container. They used a 2D transient enthalpy-porosity method in a fixed grid. They examined two different PCMs with high and low thermal conductivity in different geometrical parameters. The governing equations were natural convection equations for melted part of PCM. They have reported a correlation between melting time and void fraction. Zhao et al. [11] investigated heat transfer of encapsulated PCM for thermal energy storage. In this study, transient 2D simulation has been used to study the PCM applications in the high temperature thermal storage in solar power systems. In this study, the PCM was NaNO_3 , which is encapsulated by a stainless steel in a cylindrical capsule. The flow regime was laminar and turbulent. The method was enthalpy-porosity approach. Bayat et al. [12] studied finned heat sink performance enhancement with nanoparticles in PCM. Due to the low conductivity of PCMs, they added copper oxide and aluminum oxide nanoparticles up to 6% volume fraction to paraffin as a PCM. Their results show that adding aluminum oxide in a low volume fraction (2%) has a better performance.

One of the weak points of the PCMs is having low thermal conductivity. The effect of the pretense of internal fins in a PCM heat sink has been studied by Shatikian et al. [13]. The PCM is located between the fins, and heat is transferred from the base plate to the fins and the PCM. The top of the domain is open and is in contact with air. They simulated it by the Fluent 6.0 software and their results show the melting characteristics are depending on the thermal properties of the PCM and the geometrical parameters. Aziz et al. [14] studied the PCM behavior in a spherical capsule. Since the main weakness of the PCMs is their low thermal conductivity, they used metal fins to improve the thermal conductive coefficient of the PCMs in different shell materials. Their results show that using the copper coating with fins reduces the melting time by 37%. Thermal energy storages need a material with high heat capacity. The PCM in the phase change time, rules as a fluid with high heat capacity. Mourad et al. [15] modeled the nano-enhanced paraffin wax as PCM by the enthalpy-porosity method. They showed that the nanoparticles reduced the melting time by 62% compared with the base case.

As mentioned in the above works [1-15], PCMs are useful to save energy and release it at

the needed times. This is due to the large isothermal specific heat capacity.

In this paper, heat transfer and fluid flow in a channel equipped with two pipes containing PCM have been studied numerically. The optimum size and location of the pipes were obtained in the previous work [16]. Change in the phase change material temperature depends on various parameters, including phase change material to fluid flow properties ratios such as thermal conductivity, specific heat capacity, and the Grashof number of the PCM. Then, for simulation, the effect of buoyancy force in the pipes, the effects of PCM on heat transfer flow conductivity ratio (k_r), their special heat capacity ratio (Cp_r), and Grashof number were studied. Defining the discharging time of the PCM in different parameter values (k_r , Cp_r , Gr) is important, as it needs to be charged again before heat transfer vanishes. In comparison with the previous work [16], in the last work, the PCM was in the phase change duration with constant temperature. But, in this study, the PCM is fully melted, and its temperature increases over time. Then, in this study, the effects of buoyancy force in different k_r , Cp_r , and Gr on the discharging time of the PCM have been studied. Discharging time is a time which the PCM should leave the system to be charged after reaching the temperature of the passing fluid. An application of this topic is in air-conditioning, which uses ice in the pipes as PCM for coolant and the aim is calculating the PCM discharging time. The longer the discharge time, is favorable in using encapsulated PCM in air conditioning and other applications such as CPUs cooling.

2. Governing Equations and Boundary Conditions

The geometry of a vertical channel which equipped by two cylinders containing PCM is shown in Fig. 1. The flow is laminar, unsteady, incompressible and two dimensional. The optimum diameter (D) and situation (B) of the PCM containers have been obtained in the previous study [16] and are $d=D/H=0.165$ and $b=B/H=0.175$, as used in this study.

Due to symmetry, the solution domain starts at a boundary of the channel wall and continues to the center of the channel. The grid generation strategy in the fluid flow domain has been explained in the previous study [16] and in the PCM (pipe) avoiding singularity in the center of the pipe, is made of two parts. One part is a uniform with Cartesian mesh in the center of the pipe and the other one is an O-type grid. These domains have overlaps and the results of the overlaps are used as a boundary condition for both parts.

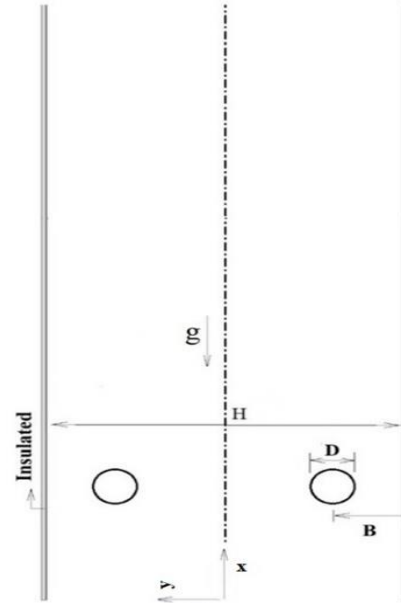


Fig. 1. The geometry of the vertical channel with two pipes containing PCM

Fig. 2 shows the generated grid. In this figure the mesh is more compress near the channel and pipe walls.

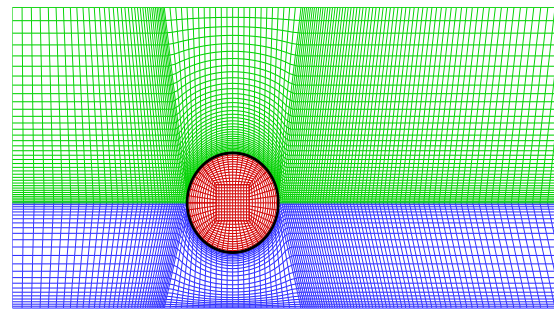


Fig. 2. Generated mesh both in the main flow and in the pipe (PCM)

Because of the body fitted grid (Fig. 2), the governing equations should transform from the physical domain to the calculation domain [17, 18]. By introducing the following non-dimensional parameters,

$$\begin{aligned}
 x_i &= \frac{X_i}{H}, d = \frac{D}{H}, b = \frac{B}{H}, t^* = \frac{U_b t}{H}, u_i = \frac{U_i}{U_b}, \\
 p &= \frac{P}{\rho_f U_b^2}, T = \frac{\theta - \theta_{0-PCM}}{\theta_{in} - \theta_{0-PCM}}, Re = \frac{\rho_f U_b H}{\mu_f}, \\
 Pr &= \frac{\mu_f Cp_f}{k_f}, Pe = Re Pr, Cp_r = \frac{Cp_{PCM}}{Cp_f}, \\
 k_r &= \frac{k_{PCM}}{k_f}, \mu_r = \frac{\mu_{PCM}}{\mu_f}, \rho_r = \frac{\rho_{PCM}}{\rho_f}, \\
 Gr &= \frac{\rho_{PCM}^2}{\mu_{PCM}^2} \beta_{PCM} H^3 g (\theta_{in} - \theta_{0-PCM})
 \end{aligned} \tag{1}$$

the governing equations for laminar flow both in the fluid and PCM domains can be expressed as follows [17, 18],

In the fluid flow,

Continuity,

$$\frac{\partial u^c}{\partial \xi} + \frac{\partial v^c}{\partial \eta} = 0, \tag{2}$$

Momentum,

$$\frac{\partial u^c \psi}{\partial \xi} + \frac{\partial v^c \psi}{\partial \eta} = \tag{3}$$

$$JS_p + \left[\frac{\partial}{\partial \xi} \left(\frac{Jq_{11}}{Re} \psi_\xi \right) + \frac{\partial}{\partial \eta} \left(\frac{Jq_{22}}{Re} \psi_\eta \right) \right] + JS_{CD}^\psi,$$

where ψ is “u” or “v”. The first term of the right side (JS_p) is the pressure gradient and JS_{CD}^ψ is the source term appeared due to non-Cartesian mesh. Details of the other parameters such as are expressed in [17, 18].

But, energy is an unsteady equation

$$\frac{\partial T}{\partial t^*} + \frac{\partial u^c T}{\partial \xi} + \frac{\partial v^c T}{\partial \eta} = \tag{4}$$

$$\left[\frac{\partial}{\partial \xi} \left(\frac{Jq_{11}}{Pe} T_\xi \right) + \frac{\partial}{\partial \eta} \left(\frac{Jq_{22}}{Pe} T_\eta \right) \right] + JS_{CD}^T,$$

Also, the governing equations including momentum and energy are unsteady for PCM.

The unsteady governing equations for PCM, Continuity,

$$\frac{\partial u^c}{\partial \xi} + \frac{\partial v^c}{\partial \eta} = 0, \tag{5}$$

x-Momentum,

$$\frac{\partial u}{\partial t^*} + \frac{\partial u^c u}{\partial \xi} + \frac{\partial v^c u}{\partial \eta} = \frac{JS_{pu}}{\rho_r} + \tag{6}$$

$$\frac{\mu_r}{\rho_r} \left[\frac{\partial}{\partial \xi} \left(\frac{Jq_{11}}{Re} u_\xi \right) + \frac{\partial}{\partial \eta} \left(\frac{Jq_{22}}{Re} u_\eta \right) \right] + \frac{\mu_r}{\rho_r} JS_{CD}^u +$$

$$J \left(\frac{\mu_r}{\rho_r} \right)^2 \frac{Gr}{Re^2} T,$$

The buoyancy force is considered by the Boussinesq approximation for the PCM motion in the pipes.

y-momentum,

$$\frac{\partial v}{\partial t^*} + \frac{\partial u^c v}{\partial \xi} + \frac{\partial v^c v}{\partial \eta} = \frac{JS_{pv}}{\rho_r} + \tag{7}$$

$$\frac{\mu_r}{\rho_r} \left[\frac{\partial}{\partial \xi} \left(\frac{Jq_{11}}{Re} v_\xi \right) + \frac{\partial}{\partial \eta} \left(\frac{Jq_{22}}{Re} v_\eta \right) \right] + \frac{\mu_r}{\rho_r} JS_{CD}^v,$$

and energy,

$$\frac{\partial T}{\partial t^*} + \frac{\partial u^c T}{\partial \xi} + \frac{\partial v^c T}{\partial \eta} = \tag{8}$$

$$\frac{k_r}{(\rho Cp)_r} \left[\frac{\partial}{\partial \xi} \left(\frac{Jq_{11}}{Pe} T_\xi \right) + \frac{\partial}{\partial \eta} \left(\frac{Jq_{22}}{Pe} T_\eta \right) \right] + \frac{k_r}{(\rho Cp)_r} JS_{CD}^T,$$

Eqs. 4, 6, 7 and 8, are unsteady. The PCM velocity at initial time is zero and its initial

temperature is equal to the temperature of the main inlet flow.

It is supposed that the thermal conductivity of the pipe wall is high and the pipe wall is so thin. Then it doesn't need to solve the conduction heat transfer equation in the body of the pipes as a conjugate problem.

Boundary Conditions

On the channel and the pipe walls, the no-slip condition is applied and to find out the effect of the PCM presence, the channel walls have been supposed to be insulated. Due to the symmetry, in the middle of the channel the following relation has been applied,

$$\frac{\partial \psi}{\partial y} \Big|_{y=0} = 0, \tag{9}$$

where ψ denotes to the velocity components, pressure and temperature.

It is supposed that the velocity profile is fully developed before arriving the inlet boundary and will be fully developed again at the outlet boundary. Based on these explanations, the boundary conditions at inlet and outlet boundaries, are expressed as follows,

$$u(0, y) = 1.5y(1 - y), v(0, y) = 0, T(0, y) = 1, \tag{10}$$

$$\frac{\partial u}{\partial x} \Big|_{x=L^*} = 0, v(L^*, y) = 0, \frac{\partial T}{\partial x} \Big|_{x=L^*} = 0$$

In the interface boundary of the PCM and fluid flow (pipe wall) the temperature is obtained as follow and is used as a boundary condition for both the fluid flow and the PCM temperature,

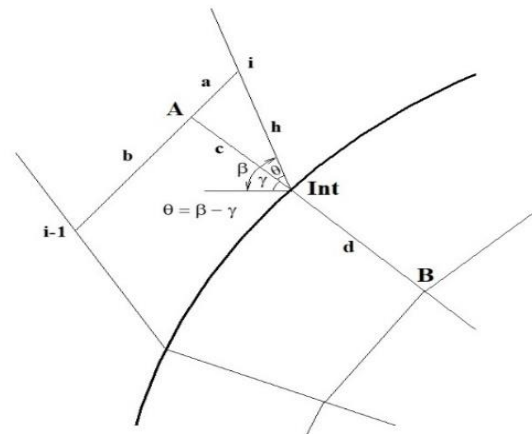


Fig. 3. The geometrical parameters to apply the main flow and PCM interface boundary condition

The continuous heat flux and temperature of the PCM and fluid flow in the interface, leads to,

$$u(0, y) = 1.5y(1 - y), v(0, y) = 0, T(0, y) = 1, \tag{11}$$

$$-k \frac{\partial T}{\partial n} \Big|_f = -k \frac{\partial T}{\partial n} \Big|_{PCM}$$

then,

$$-k_f \frac{T_A - T_{int}}{c} = -k_{PCM} \frac{T_{int} - T_B}{d} \quad (12)$$

By introducing

$$\lambda = \frac{k_{PCM} c}{k_f d} \quad (13)$$

Then,

$$T_{int} = \frac{bT_B + T_A}{\lambda + 1} \quad (14)$$

where T_A is obtained in numerical solution and, is obtained by the following interpolation,

$$T_A = \frac{bT_i + aT_{i-1}}{b + a} \quad (15)$$

In Eq. (15), T_i , T_{i-1} are obtained by numerical solution but a , b , c should be obtained by the geometrical operations. γ is obtained using the position of the node "i", β is obtained using the pipe nodes on the interface boundary and $\theta = \beta - \gamma$. Then $c = h \cdot \cos\theta$ and $a = h \cdot \sin\theta$.

3. Numerical Procedure

The governing equation has been solved by a finite volume method. The interpolation of the Rhie and Chow [19] has been applied to find the velocity component on the cell's boundaries. In the unsteady equations (4,6,7,8) which have a temporal term, the fully implicit method [20] has been used to discrete this term. Also, for convective terms, the HYBRID differencing [21] is applied. Finally, the SIMPLE method [22] used to solve the fluid flow and the PCM domains in a FORTRAN computer code written by the author.

The under-relaxation factors for x and y-momentum, pressure correction and energy equations are 0.7, 0.7, 0.1 and 0.9 respectively. Solution convergence has been checked after each time step. Because of the mesh configuration and the reasons of choosing such a body fitted mesh as described in the previous work [16] the fluid domain is made of two parts. The results of the interface have been used as a boundary condition for other part. Due to the large variation in temperature at initial times, the time step is not uniform and is small at initial times, and by time increasing, the time step grows up.

Results are based on the mean temperature of the PCM and change in the fluid bulk temperature. The temperature of the PCM is obtained by the average temperature of the PCM in the pipe,

$$T_{PCM} = \frac{4}{\pi d^2} \int_{A-PCM} T dA \quad (16)$$

and the fluid bulk temperature is obtained by the following formulas as obtained in [16],

$$T_b = 2 \int_{y=0}^{y=0.5} uT dy \quad (17)$$

The heat transfer rate from the working fluid to the PCM has been obtained as follow,

$$\frac{\dot{Q}}{k(\theta_{in} - \theta_{block})} = Pe \cdot \Delta T_b \quad (18)$$

where ΔT_b is the change in the inlet and outlet temperature of the fluid bulk temperature. Then, the $Pe \cdot \Delta T_b$ can be used to calculate the heat transfer from the fluid flow to the PCM.

The grid independency of results for $Re=700$, $Pr=3$, $b=0.175$, $d=0.165$ is carried out in the previous study [16] and the mesh with 312×52 nodes with maximum error less than 2% has been selected.

To avoid repetition, the code validity is not presented in the present paper and it has been shown in the previous work [16] by compare the results with [23-25] for air flow around the isothermal cylinder at $Re_D=40$ with the maximum error 2%.

4. Results and Discussion

One of the optimum states obtained in the previous study [16] is $Re=700$, $Pr=300$, $d=0.165$, $b=0.175$. The following results are reported based on this state. The effective parameters in this study are Cp_r , Gr , k_r , ρ_r and μ_r . The default parameters are $Cp_r = 10^4$, $Gr = 2 \times 10^4$, $k_r = 1$, $\rho_r = 1$, $\mu_r = 1$. The results are presented to report the needed time for PCM temperature to reach the 0.99 of the fluid inlet temperature (discharge time) and the change in the fluid bulk temperature. The results will be presented to find out the effects of the Cp_r , Gr , k_r on the discharge time of the PCM.

In Fig. 4, the streamlines for different times in the fluid flow and in the pipe (filled with PCM) have been shown for $Cp_r = 10^4$, $Gr = 2 \times 10^4$, $k_r = 1$, $\rho_r = 1$, $\mu_r = 1$. It is clear from the governing Eqs. (2, 3) that the results of the fluid flow are just depend on the Reynolds number. Then the streamlines in the Fig. 4 which is plotted for $Re=700$ are same for different times. In the other hand, the fluid flow domain results are time independent. In this figure, the streamlines in the PCM due to buoyancy force for different times are shown. By time increasing the effect of the inlet temperature on the PCM temperature will be more sensible and it will affect the circulation velocity of the PCM and its streamlines.

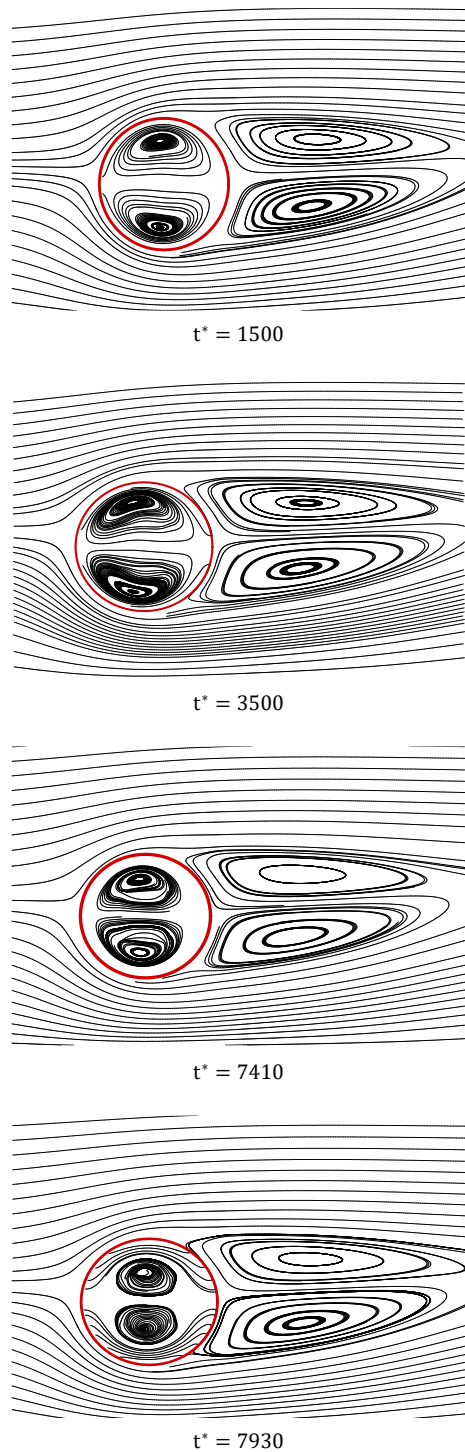


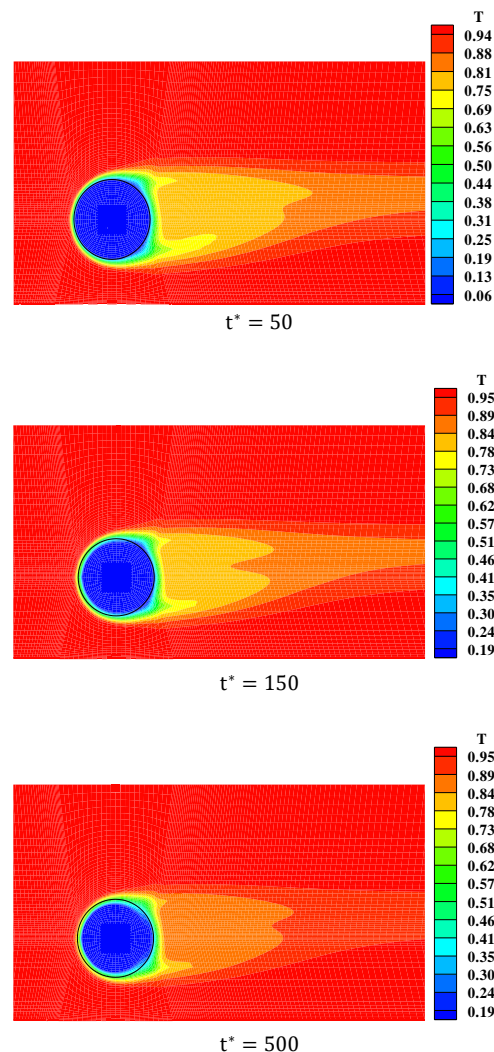
Fig. 4. Streamlines both in the main flow and PCM at different times

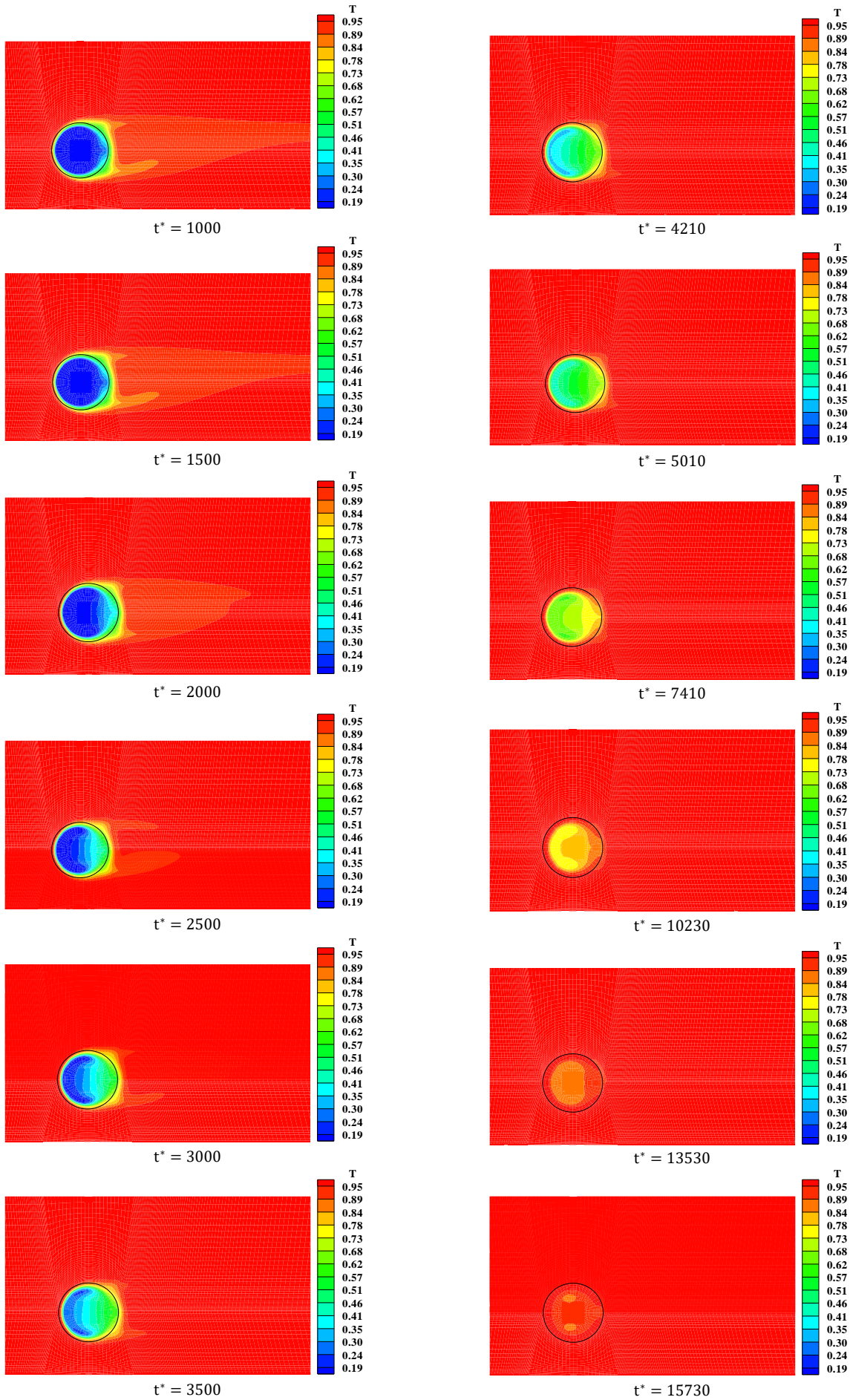
As expressed from Eqs. (4, 6, 7, 8) the temperature of the fluid and the PCM are time dependent. Fig. 5, shows the time dependent temperature of the PCM and the fluid flow for $Cp_r = 10^4, Gr = 2 \times 10^4, k_r = 1, \rho_r = 1, \mu_r = 1$. It is supposed that the PCM phase change duration (constant temperature) has been finished and then, its temperature increases by time.

For the initial times the temperature of the PCM is the melting temperature (T_{0-PCM}). By time increasing, the PCM temperature is influenced by

the temperature of the working fluid. For the initial times the situation of the minimum temperature of the PCM is closer to the right side of the pipe. By time increasing this point moves toward the left side. This is due to the effect of the buoyancy force. By time increases, this parameter which is introduced by Grashof number has more effect on the PCM velocity components. By more increasing in time, the temperature of the PCM will be more uniform due to effect of the mixing, caused by the buoyancy force.

Such as the PCM temperature, the temperature of the fluid flow varied by time, due to change in the pipe wall temperature. In the other hand, the PCM get heat from the fluid flow and its temperature will increase. The increased temperature of the PCM which is act as a boundary condition for the working fluid temperature causes increase in the working fluid temperature. Approaching the final times, the temperature of the PCM and outlet flow will be close to the inlet temperature. In summary, change in the temperature of the fluid flow and PCM are more sensible in the initial times and by time increasing the rate of temperature change decreases.





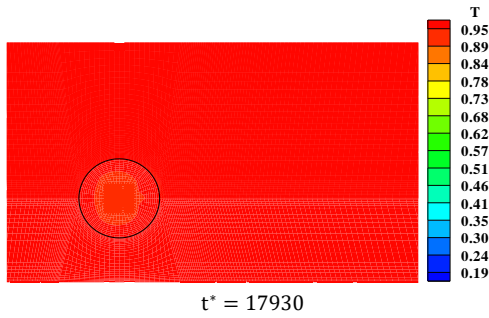


Fig. 5. Streamlines both in the main flow and PCM at different times

The effects of the effective parameters including specific heat capacity ratio, thermal conductivity ratio and the Grashof number on the temperature of the PCM and the heat transfer rate from the fluid flow to the PCM is depicted in Figs. 6-8.

Fig. 6 shows the temperature variation of the PCM and the working fluid by time. It has been shown that the temperature variations at initial times is high. By time increasing, this variations rate will decrease. It is due to temperature increasing of the PCM which reduces the heat transfer between the PCM and the working fluid. By increase in specific heat capacity ratio the temperature increasing rate decreases and the temperature of the PCM increases slowly. This behavior is also, visible in the fluid flow temperature increasing as a function of the specific heat capacity ratio. The rate of the temperature increasing at the first step times is high but by approaching to the final times, the temperature increasing steep will decrease. Because, in general, this heat transfer is in the sensible domain and by increase in “ Cp ” ratio, it is obvious that the increasing temperature rate will decrease. The change in the working fluid temperature is a little complicated at initial times (less than 4,000).

Then the needed time for the PCM temperature to reach 0.99 is higher for lower Cp_r . This trend of changing the temperature can be seen in the results of [3, 8]. The results show that the discharging time is 11,000 for $Cp_r=10^3$ and 28,000 for $Cp_r=10^4$. It is clear that by time spending, the temperature of the PCM increased due to get heat from the main fluid flow.

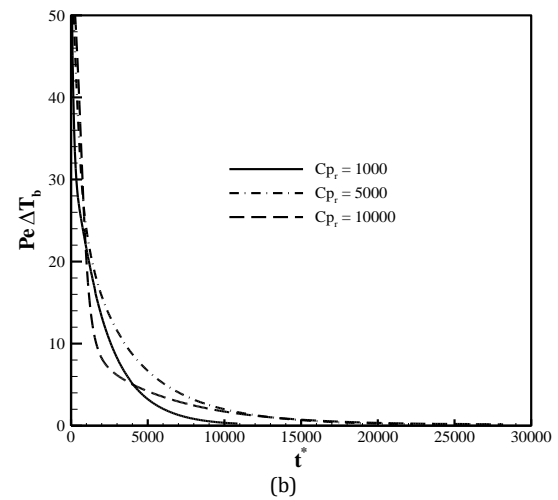
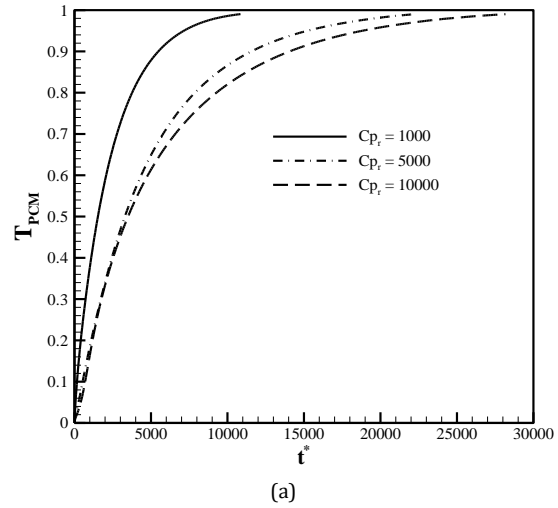


Fig. 6. (a) the mean temperature of PCM and (b) the fluid bulk temperature variation at different specific heat capacity ratio number vs. time

Effect of “ k_r ” is shown in Fig. 7. This parameter has effect on the problem as can be seen in Eqs (8, 13). It has been shown that by increase in this ratio, the temperature of the PCM increases in a shorter time. It is due to increase in diffusion terms in Eq. (8) for the PCM temperature. Also, the change in the working fluid decreases by increase in this parameter due to reduction in diffusion terms in Eq. (8). Then the needed time for the PCM temperature to reach 0.99 is higher for lower k_r . The results show that the discharging time is 25,000 for $k_r=0.5$ and is 34,000 for $k_r=1.5$.

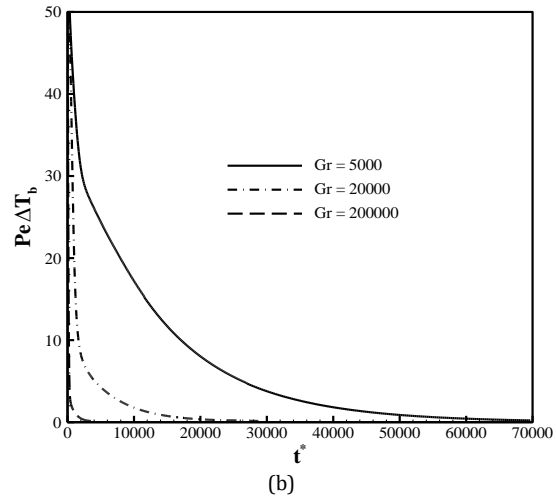
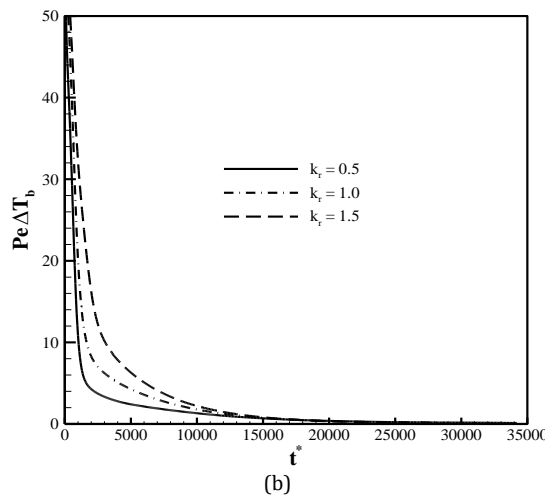
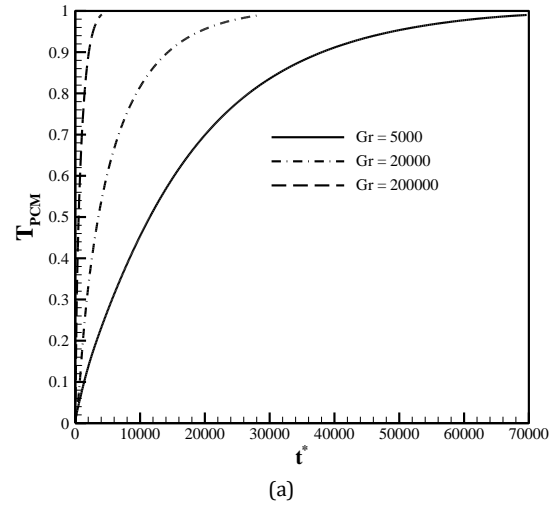
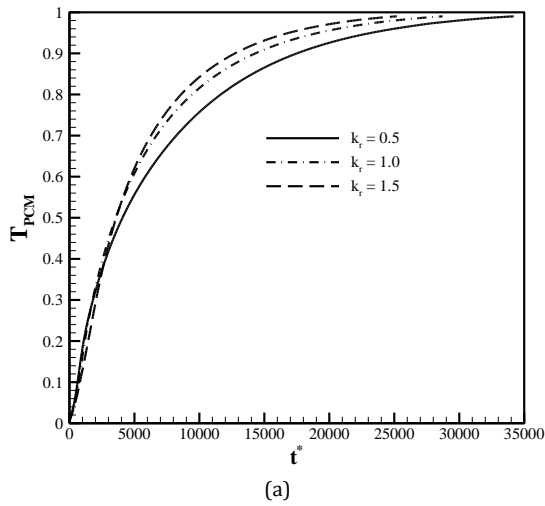


Fig. 7. (a) the mean temperature of PCM and (b) the fluid bulk temperature variation at different thermal conductivity ratio number vs. time

Fig. 8. (a) the mean temperature of PCM and (b) the fluid bulk temperature variation at different Grashof number vs. time

The effect of the Grashof number is illustrated in Fig. (8). It is shown that for higher Grashof number the temperature increasing for PCM is occurred in the shorter times. It is due to the better mixing of PCM which created the free convective heat transfer mechanism. In this mechanism both conduction in diffusion and the convective terms in the energy equation are cooperating in the heat transfer between the PCM and the working fluid. Then the needed time for the PCM temperature to reach 0.99 is lower for higher Gr. The results show that the discharging time is 4,000 for Gr=5,000 and is 70,000 for Gr=200,000.

In high Grashof number and high “ k_r ”, the results are expected to be closer to the results of the lumped temperature assumption. High “ k_r ” will occur when the PCM is equipped by the metal porous medium with high thermal conductivity. In the high Grashof number the results can approach the results of the lumped temperature assumption for the PCM. This phenomenon can be seen in Fig. (9). It is due to favorable mixing effects in the PCM which lead the PCM temperature to be lumped. It can be seen that the results are adjusted approximately. Also, it can be concluded that the porous media used to increase the k_r will eliminate the effect of the buoyancy.

Then to achieve the same results it needs to use a porous media with high thermal conductivity. But, executing the computer code for the pure conduction with $k_r = 100$ leads to the results as same as the results for $k_r = 50$. It means that the increase in k_r has a limited effect on heat transfer to the PCMs. Finally, it can be seen, that in the beginning times the result of the lumped temperature assumption has different with the result of buoyancy model. Because, at the beginning time the PCM doesn't mix well and its temperature is not uniform.

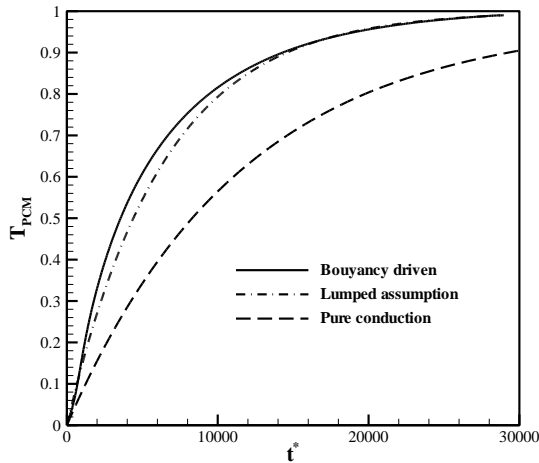


Fig. 9. A comparison of high buoyancy effect ($Gr = 2 \times 10^4, k_r = 1$) and high conductivity effect ($Gr = 0, k_r = 50$) and lumped temperature assumption, for mean temperature of PCM

5. Conclusions

One way to reduce energy consumption in buildings is to use PCM. In air conditioning, the chiller can turn on in midnight when the electricity consumption is minimum to make ice in the capsules. At the morning, only the fan of the air conditioner (with low electricity consumption) is turned on to pass air through these capsules and provide the needed cool air for the building. The aim is calculating the PCM discharging time. In this paper, a channel equipped by two pipes filled with PCMs has been studied numerically. The governing equation including continuity, momentum and energy in both the PCM and the working fluid have been solved by control volume method (SIMPLE) in curvilinear coordinate.

The problem simulated after melting point for PCM when its temperature increased by heat getting from the outer fluid flow. The buoyancy driven is considered and modeled by the Boussinesq approximation. The effects of the important parameters such as PCM to the working fluid specific heat capacity ratio, thermal conductivity ratio and the Grashof number have been studied. It has been found that in higher Grashof number due to well PCM mixing, the heat

transfer rate from the working fluid to the PCM increased. Also, the effect of the thermal conductivity ratio, shows that in higher thermal conductivity for the PCM, the heat transfer rate is high. It is because of the improvement in diffusion terms in the energy equation. Finally, the effect of the specific heat capacity ratio shows that in higher ratio, the temperature increasing rate of the PCM reduces.

The results show that the nondimensional discharging time is 4,000 for $Gr=5,000$ while is 70,000 for $Gr=200,000$. It is 25,000 for $k_r=0.5$ while is 34,000 for $k_r=1.5$. Also, it is 11,000 for $C_{p_r}=10^3$ while is 28,000 for $C_{p_r}=10^4$. In some situations, such as in high Grashof number, due to well mixing, the temperature of the PCM can be supposed to be lumped. Also, in the beginning time, when the PCM is not well mixed, the results differ from the results of the lumped temperature assumption.

Nomenclature

b, B	The distance of the pipe from the wall [m]
C_p	Specific heat capacity [J/kg.K]
d, D	Diameter [m]
g	Gravity [m/s ²]
Gr	Grashof number
H	Height of the channel [m]
k	Thermal conductivity [W/mK]
L	Channel length [m]
m	Mas [kg]
\dot{m}	Flow mass rate [kg/s]
p, P	Pressure [Pa]
Nu	Nusselt number
Pe	Peclet number
Pr	Prandtl number
\dot{Q}	Heat transfer rate [W]
Re	Reynolds number
Re_D	Reynolds number based on "D"
t	Time [s]
T	Temperature [K]

U,V	Velocity components [m/s]
u,v	Nondimensional velocity components
X,Y	x,y coordinate [m]
x,y	Nondimensional X, Y
Greek Symbol	
β	Thermal expansion coefficient [1/K]
ξ, η	Curvilinear coordinate components
θ	Temperature, [K]
μ	Viscosity, [Pa.s]
ρ	Density [kg/m ³]
ψ	General velocity components [m/s]
Superscripts	
c	Contravariant velocities
*	Nondimensional time and length
Subscripts	
b	Fluid bulk value
f	Fluid
in	Interface
out	Outlet
PCM	Phase change material
R	PCM to working fluid properties ratio
0	Value at the initial time

Funding Statement

This research did not receive any specific grant from funding agencies in the public, commercial, or not-for-profit sectors.

Conflicts of Interest

The author declares that there is no conflict of interest regarding the publication of this article.

References

[1] Ho, C.J. and Cheng, Y.T., 1999. On cooling behavior of a vertical plate in a phase change material/water composite enclosure under pulsating heat load. *Heat and mass transfer*, 34(6), pp.509-515.

[2] Yan, S.R., Fazilati, M.A., Samani, N., Ghasemi, H.R., Toghraie, D., Nguyen, Q. and Karimipour, A., 2020. Energy efficiency optimization of the waste heat recovery system with embedded phase change materials in greenhouses: a thermo-economic-environmental study. *Journal of Energy Storage*, 30, p.101445

[3] Khan, R. J., Bhuiyan, Md. Z. H., Ahmed, D. H., 2020, Investigation of heat transfer of a building wall in the presence of phase change material (PCM). *Energy and Built Environment*, 1, pp. 199-206.

[4] Khodadadi, J. M., Zhang, Y., 2001, Effects of buoyancy-driven convection on melting within spherical containers. *International Journal of Heat and Mass Transfer*, 44, pp. 1605-1618.

[5] Assis, E., Katsaman, L., Ziskind, G., Letan, R., 2007, Numerical and experimental study of melting in a spherical shell. *International Journal of Heat and Mass Transfer*, 50, pp. 1790-1804.

[6] Tan, F. L., Hosseinizadeh, S. F., Khodadadi, J. M., Fan, L., 2009, Experimental and computational study of constrained melting of phase change materials (PCM) inside a spherical capsule. *International Journal of Heat and Mass Transfer*, 52, pp. 3464-3472.

[7] Elmozughi, A. F., Solomon, L., Oztekin, A., Neti, S., 2014, Encapsulated phase change material for high temperature thermal energy storage Heat transfer analysis. *International Journal of Heat and Mass Transfer*, 78, pp. 1135-1144.

[8] Aadmi, M., Karkri, M., Hammouti, M. E., 2015, Heat transfer characteristics of thermal energy storage for PCM (phase change material) melting in horizontal tube: Numerical and experimental investigations. *Energy*, 85, pp. 339-352.

[9] Zeneli, M., Malgarinos, I., Nikolopoulos, A., Nikolopoulos, N., Grammelis, P., Karellas, S., Kakaras, E., 2019, Numerical simulation of a silicon-based latent heat thermal energy storage system operating at ultra-high temperatures. *Applied Energy*, 242, pp. 837-853.

[10] Mallya, N., Haussener, S., 2021, Buoyancy-driven melting and solidification heat transfer analysis in encapsulated phase change materials. *International Journal of Heat and Mass Transfer*, 164, 120525.

[11] Zhao, W., Elmozughi, A. F., Oztekin, A., Neti, S., 2013, Heat transfer analysis of encapsulated phase change material for

- thermal energy storage. *International Journal of Heat and Mass Transfer*, 63, pp. 323-335.
- [12] Bayat, M., Faridzadeh, M. R., Toghraie, D., 2018, Investigation of finned heat sink performance with nano enhanced phase change material (NePCM). *Thermal Science and Engineering Progress*, 5, pp. 50-59.
- [13] Shatikian, V., Ziskind, G., Letan, R., 2005, Numerical investigation of a PCM-based heat sink with internal fins. *International Journal of Heat and Mass Transfer*, 48, pp. 3689-3706.
- [14] Aziz, S., Amin, N. A. M., Abdul Majid, M. S., Belusko, M., Bruno, F., 2018, CFD simulation of a TES tank comprising a PCM encapsulated in sphere with heat transfer enhancement. *Applied Thermal Engineering*, 143, pp. 1085-1092.
- [15] Mourad, A., Aissa, A., Abed, A. M., Smaisim, G. F., Toghraie, D., Fazilati, M. A., Younis, O., Guedri, K., Alizadeh, A., 2022, The numerical analysis of the melting process in a modified shell-and-tube phase change material heat storage system. *Journal of Energy Storage*, 55D, 105827.
- [16] Rostami, J., 2020, Optimum Diameter and Location of Pipes Containing PCMs in a Channel in Latent and Sensible Heat Transfer. *AUT Journal of Mechanical Engineering*, 4, pp. 551-559.
- [17] Hoffman, K. A., 1989, *Computational Fluid Dynamics for Engineers*, Engineering Education System, Austin, Texas.
- [18] Raisee, M., 1999, *Computation of Flow and Heat Transfer Through Two- and Three-Dimensional Rib-Roughed Passages* (Doctoral Thesis, University of Manchester).
- [19] Rhie, C. M., Chow, W. L., 1983, Numerical Study of the Turbulent Flow Past an Airfoil with Trailing Edge Separation. *AIAA J.*, 21 (11), pp. 1525-1535.
- [20] Versteeg, H. K., Malalasekera, W., 2007, *An Introduction to Computational Fluid Dynamics: The Finite Volume Method*, Harlow, England: Pearson Education Ltd.
- [21] Spalding, D. B., 1972, A Novel Finite Difference Formulation for Differential Expressions Involving Both First and Second Derivatives. *International Journal for Numerical Methods in Engineering*, 4, pp. 551-559.
- [22] Patankar, S. V., Spalding, D. B., 1972, A Calculation Procedure for Heat, Mass and Momentum Transfer in Three-Dimensional Parabolic Flows. *International Journal of Heat and Mass Transfer*, 15, pp. 1787-1806.
- [23] Taira, K., Colonius, T., 2007, The immersed boundary method: A projection approach. *Journal of Computational Physics*, 225, pp. 2118-2137.
- [24] Bejan, A., 2013, *Convection Heat Transfer*, John Wiley & Sons, Hoboken, New Jersey, 4th ed.
- [25] Holman, J. P., 1997, in: *Heat Transfer*, eighth ed. McGraw-Hill Inc., New York, pp. 218-282.